Two-Phase Flow Pattern, Heat Transfer, and Pressure Drop in Microchannel Vaporization of CO_2

Jostein Pettersen / Armin Hafner

Norwegian University of Science and Technology
Trondheim – Norway

Content

- Background and purpose of study
- Experimental method
- Flow visualization results
- Heat transfer and pressure drop data
- Dry-out issues
- Correlation of heat transfer and pressure drop
- Maldistribution
- Conclusions

MOTIVATION:
What are the consequences for the heat exchanger design?

Transcritical CO_2 cycle with internal heat exchange

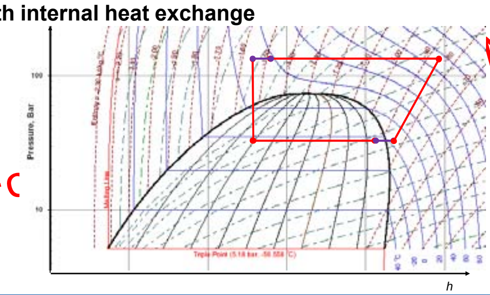

Properties of saturated CO_2

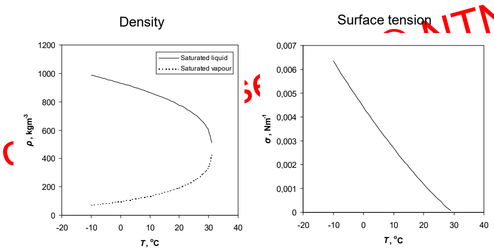

Flow pattern recordings

- Tube diameter 0.98 mm
- Digital video recorded at 4000 frames/s (fps)
- Observation from an angle of 28° from above
- Play-back at 10 fps
- Each test recorded at stable operating conditions

- T = 20°C
- q = 13 kWm^{-2}

- G = 250 and 380 kgm^{-2}s^{-1}

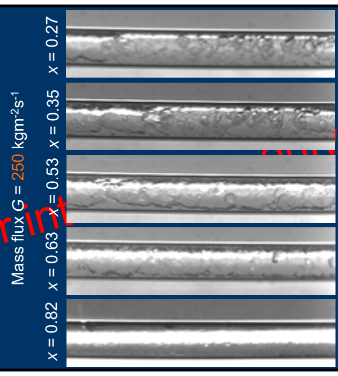

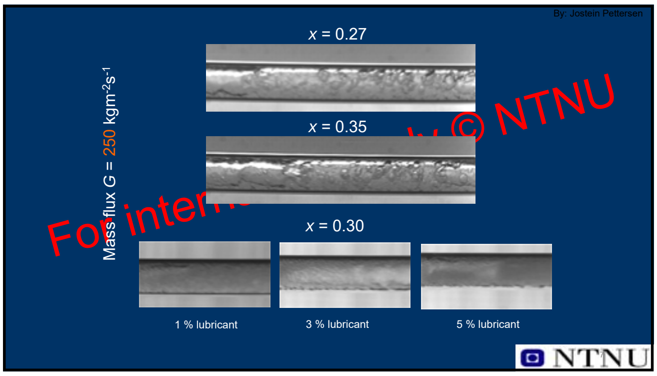

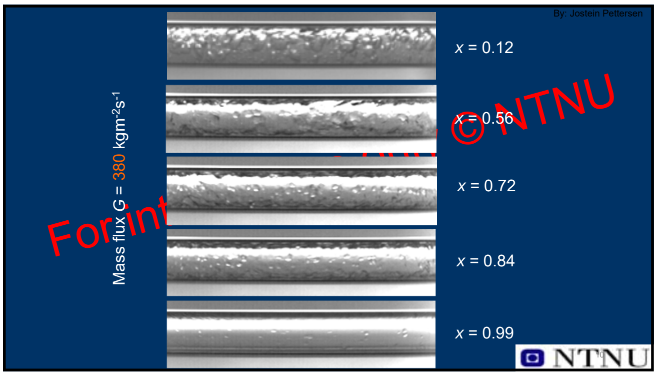

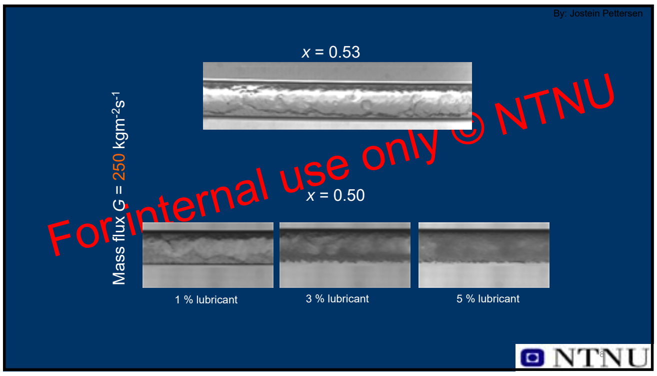

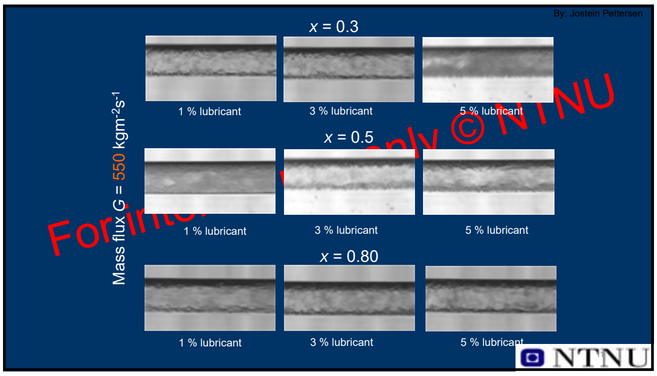

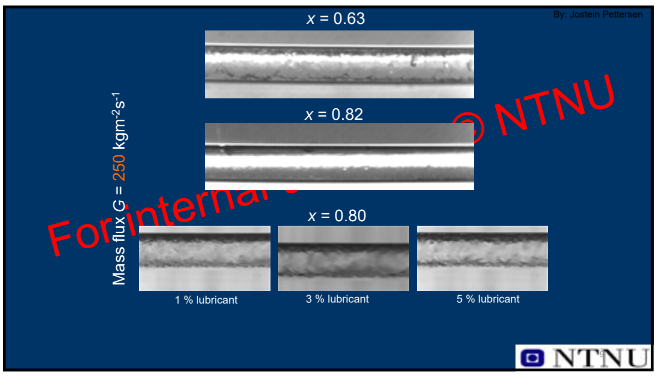

Flow regime maps

Based on all observations at T=20°C. Approximate transition lines

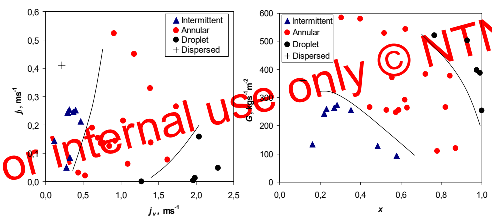

- Stratified flow not observed (q > 0)
- Generalised transition lines from literature did not fit observed regimes
- Transition to annular flow observed at very low superficial velocity

Conclusions flow visualization

- Flow pattern observations with pure CO_2 were dominated by intermittent flow at low vapour fractions, and wavy annular flow with entrainment of droplets at higher vapour fractions. Did not match predicted flow pattern maps.
- With lubricant Reniso 85E (1, 3, 5%) , almost every test shows a film flowing annulus along the tube wall. This film was assumed to consist mainly of oil. Thicker at higher oil concentrations.
- Intermittent flows are more dominant at smaller mass fluxes whereas only annular flow was observed at a higher mass flux of 550 kg/m2s. Elongated vapour bubbles seemed to be coated with an oil film. This would tend to increase the surface tension and thus decrease the heat transfer coefficient.
- Observed flow patterns are quite similar with tests, made with pure CO_2
- In tests made with oil, no entrainment was found, which however does not necessarily mean that there was no entrained droplets in the flow.
- The material should be closer studied before final conclusions are made

Geometry of heat transfer test tube

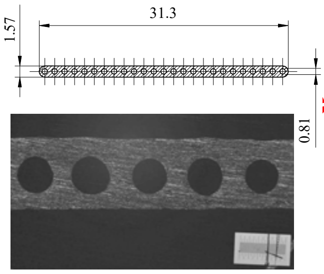

- Equivalent to tubes used in prototype heat exchangers
- Extruded from aluminium alloy
- 25 flowchannels
- Length 540 mm
- Heated length 503.4 mm
- Tests conducted with <u>horizontal</u> tube

Heat transfer test section design

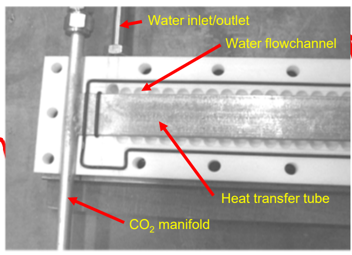

Local heat transfer data of Hihara and Tanaka (2000)

D = 1 mm, *T* = 15°C

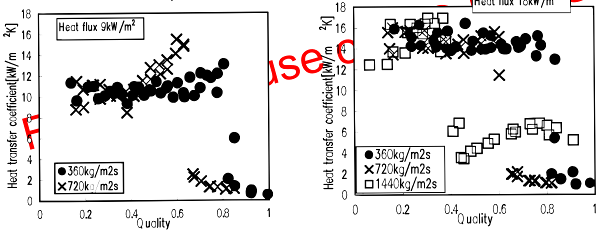

Flow visualization test rig

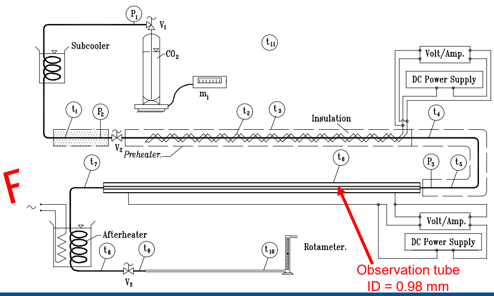

Test conditions
Flow vaporization experiments

Parameter	Symbol	Unit	Range
Mass flux	G	$kgm^{-2}s^{-1}$	190 - 570
Heat flux	q	Wm^{-2}	5,000 – 20,000
Evaporating temperature	T	°C	0 - 25

Heat transfer test data
Varying heat flux, T = 10°C

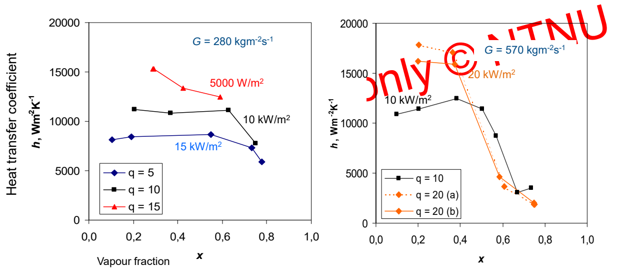

Heat transfer test data
Varying mass flux, q = 10 kWm^{-2}

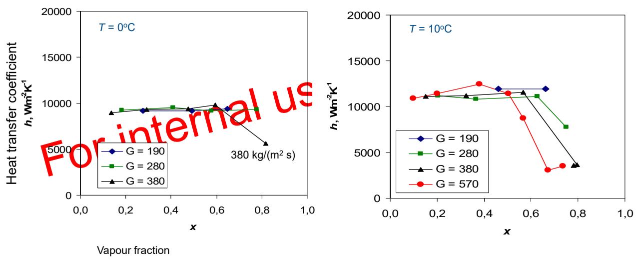

Heat transfer test data
Varying temperature

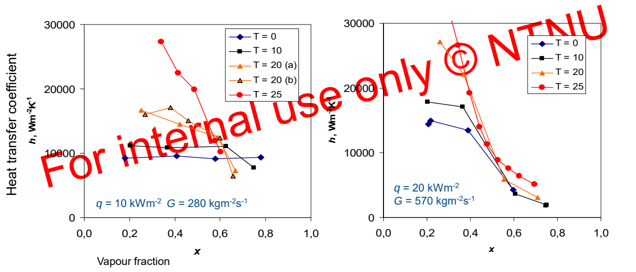

Friction pressure drop test data
Varying mass flux and temperature

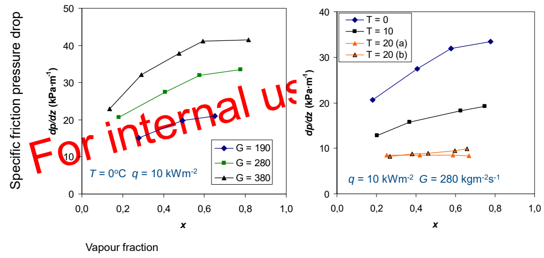

Pressure drop & heat transfer
T = 0°C q = 10 kWm^{-2}

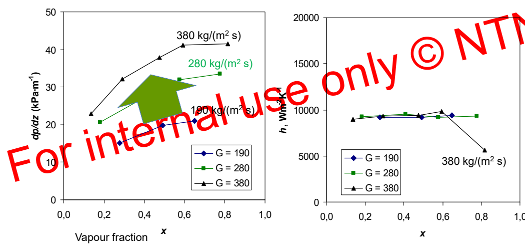

Note: Increased mass flux does not improve heat transfer but gives higher pressure drop

Pressure drop & heat transfer
T = 10°C q = 10 kWm^{-2}

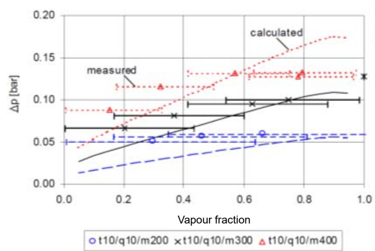

Dryout vs Departure from Nucleate Boiling (DNB)

- Dryout is CHF due to discontinuation of the liquid film on the tube wall, usually in annular flow
  - in low/medium-x flow due to disruption of liquid layer caused by surface wave instability
  - in high-x annular flow caused by dryup of the liquid layer on the heating wall due to entrainment and vaporization
- Dryout is not to be confused with DNB (Departure from Nucleate Boiling), which is a film boiling phenomenon
- DNB: Increased G gives higher turbulence, improved bubble transport and **higher** CHF
- Dryout: Increased G gives more entrainment and **reduced** CHF (lower x_{cr})

Correlation of heat transfer data

Mechanism	Model
Nucleate boiling	Cooper (1984) Gorenflo (1983)
Convective evaporation	Kattan et al. (1998)[a]
Model for combining nucleate and convective heat transfer	Asymptotic model[b], with $n = 3$
Dryout inception	Kon'kov (1965) data scaled from H_2O to CO_2 using Ahmad (1973)[c]
Post-dryout heat transfer	Shah and Siddiqui (2000)

a: $h_{ce} = 0.0133 \; Re_l^{0.69} \; Pr_l^{0.4} \; \frac{k_l}{\delta}$

b: $h = \left\{ (h_{nb})^n + (h_{ce})^n \right\}^{1/n}$

c: Using scaling factor based on Weber-Reynolds number or Barnett number

Best combination: Cooper (1984) nucleate boiling correlation, and Barnett number version of Ahmad (1973) scaling factor

Correlation of heat transfer data

Calculated mean heat transfer coefficients based on 10 points between measured inlet and outlet vapour fraction

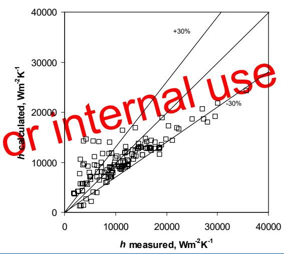

- Average deviation +7.7%
- Mean deviation 35.1%
- Overprediction when model predicts too high x_{cr}
- Underperdiction due to Cooper (1984) nucleate boiling correlation
- Change to Gorenflo (1993) correlation gave significant overprediction, and average/mean deviation of approx. 50%
- Convective contribution may be too high

Comparison of heat transfer model and experimental data

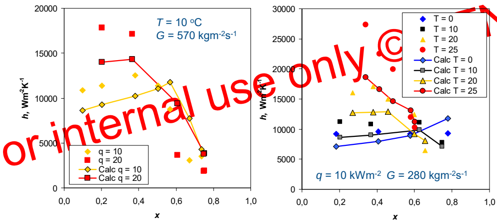

Earlier dryout than predicted may be due to flow oscillation in parallel flowchannels

Friction pressure drop

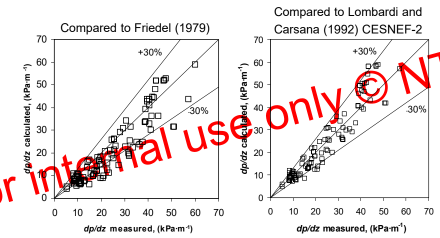

	Friedel (1979)	Lombardi and Carsana (1992)
Mean deviation:	22.3%	16.4%
Average deviation:	-17.4%	-1.1%

Underprediction at low mass flux and low temperature

Conclusion 'evaporation' inside micro channels

- Intermittent and annular flow regimes dominate
- Droplet (entrained) flow important at high mass flux
- Reduced and irregular film thickness may give dryout and reduced heat transfer even at moderate vapour fraction
- Observed two-phase flow regime transitions were not predicted well by existing models and generalized flow charts
- Extreme variation in measured CO_2 heat transfer coefficient
  - Nucleate boiling dominates prior to dryout
  - Non-equilibrium effects in post-dryout heat transfer
  - Combination of models for nucleate boiling, convective evaporation, dryout, and post-dryout heat transfer is needed

Conclusion (evap. cont.)

- Influence of lubricant may be significant and has to be investigated
- Design advice for microchannel evaporators (T > 0°C):
  - **Use low mass flux** – heat transfer remains unchanged, pressure drop is reduced, and critical vapour fraction is increased
  - **Use liquid (over)feeding** – assures nucleate boiling, reduces flow distribution problems, avoids dryout/post-dryout heat transfer

Temperature measurements

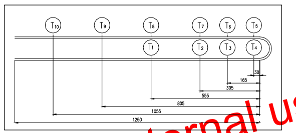

Thermocouples (Type E) are made of 0.07 mm constantan/chrome wire, soldered together and embedded in 0.5 mm deep and 80 mm long slits (Fig. below). Electrically insulating, thermally conductive epoxy and firmly pressed indium were used to ensure optimum contact between thermocouples and the tube wall, and to avoid the disturbance of heat transfer between heating cables.

Temperatures are measured at ten locations unequally distributed over the length of the test section.

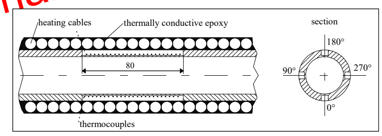

7 mm diameter aluminium tube

Test Facility

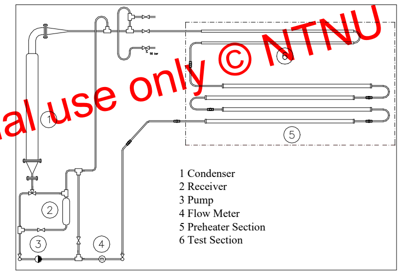

Tube wall temperature at various heat fluxes on different points of temperature measurement

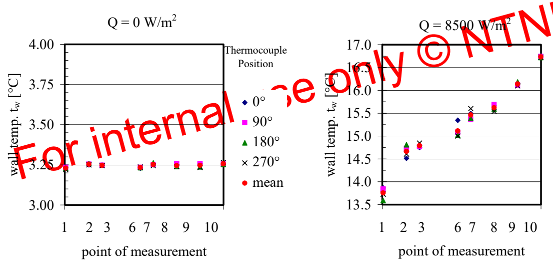

The **design of the test rig** is based upon technology and experience developed in our laboratory for experimental research on heat transfer and pressure drop, by:

1. using a fully instrumented test section consisting of two 1250 mm long horizontal smooth tubes, connected by a vertical 180° bend (r = 25 mm), to represent the typical part of an evaporator. **The inner diameter of the tube is 7 mm** and the wall thickness is 1.5 mm.
2. using a **preheater to secure fully developed flow** of defined vapour fraction into the measuring section, to secure stable measurements at different points along the evaporating process.
3. using **electrical heating to provide a known specified heat flux** in the test section, so that local heat transfer coefficients may be found by measuring the temperature difference between the tube wall and the evaporating refrigerant at locations of known pressure and vapour fraction.

Measured heat transfer coefficient, t_{sat} = -10 °C; G = 200 kg/m²; Q = 6000 W/m².

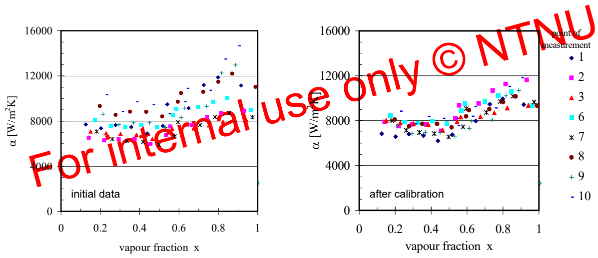

Measured heat transfer coefficient

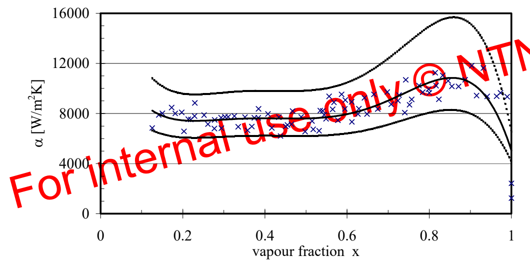

error interval with a random error in the temperature measurement of +/- 0.18 K. (t_{sat} = -10 °C; G = 200 kg/m²; Q = 6000 W/m²).

Influence of varying saturation temperature

t_{sat} = -25°C

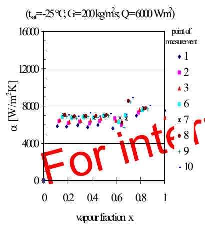

t_{sat} = -10°C

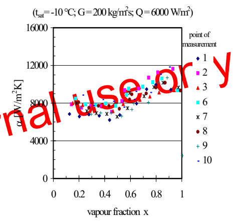

t_{sat} = 5°C

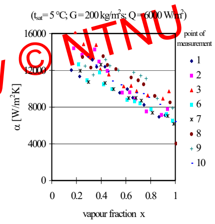

+5 °C, → completely new variation, where the heat transfer is decreasing constantly; from a very high value of around 14.000 W/m²K at vapour fraction 0.2, to a value around 8.000 W/m²K near to 1.0.

Influence of varying heat flux (heat transfer coefficient)

Q = 3 kW/m²

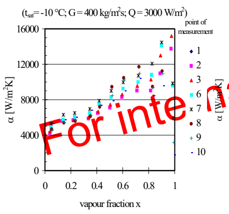

Q = 6 kW/m²

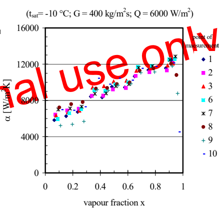

Q = 9 kW/m²

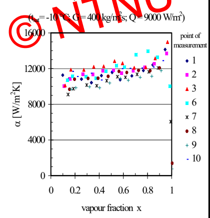

increasing heat flux at a high mass velocity (400 kg/m²s) is changes the pattern from a convective to a nucleate boiling regime

Influence of varying heat flux (pressure drop)

Q = 3 kW/m²

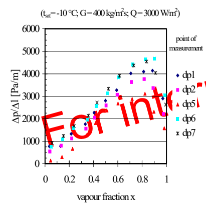

Q = 6 kW/m²

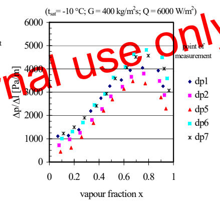

Q = 9 kW/m²

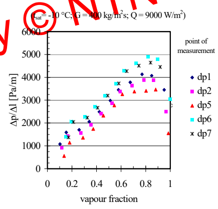

Influence of varying mass flux

G = 200 kg/m²s

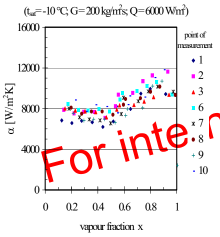

G = 300 kg/m²s

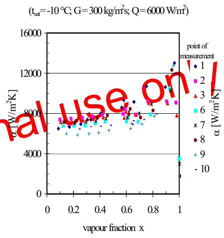

G = 400 kg/m²s

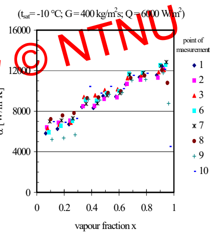

nucleate boiling has a strong effect at lower mass fluxes, so that only a small increase in heat transfer is gained from increasing the mass velocity from 200 to 300 kg/m²s.

Influence of varying mass flux

G = 200 kg/m²s

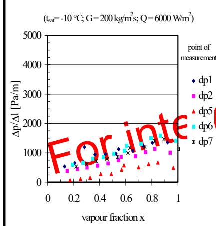

G = 300 kg/m²s

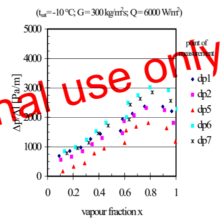

G = 400 kg/m²s

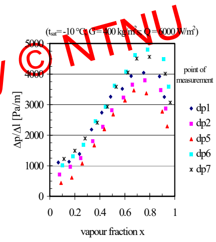

Influence of varying saturation temperature

t_{sat} = -25°C t_{sat} = -10°C t_{sat} = 5°C

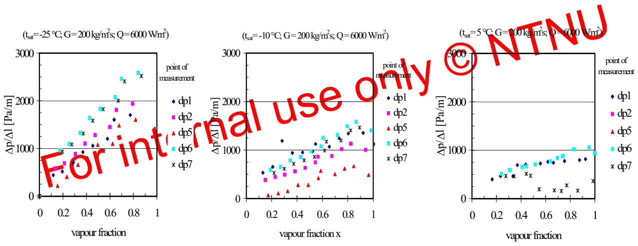

..

Heat transfer at various mass fluxes [kg/(m²s)]

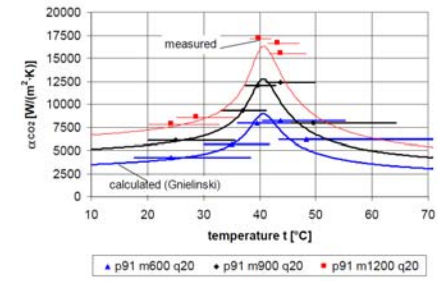

The influence of the mass flux on the heat transfer coefficient of CO_2 is significant.
If the mass flux is increased from 600 to 900 kg/(m²s) the calculation as well as the measurement show a rise in the heat transfer coefficient of about 40%, and a rise of about 80% if the mass flow is increased to 1200 kg/(m²s).

The peak in the graph indicates the pseudocritical temperature. At 91 bar the maximum c_p is located at 40.6°C.

Measured pressure drop and the Fuchs-Correlation

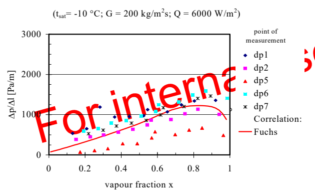

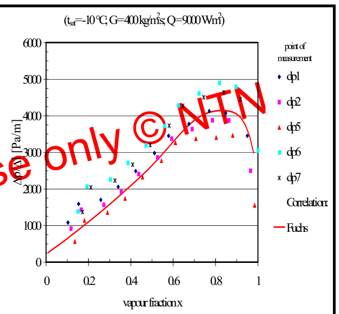

Fuchs, P. H., 1975,"Trykkfall og varmeovergang ved strømning av fordampende væske i horisontale rør og bend", Dr. Lic. grad, Department of Refrigeration, NTH, Trondheim, Norway.

Influence of heat flux to the heat transfer coefficient (10 or 20 kW/m²)

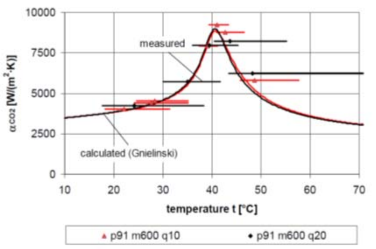

The influence of varying heat flux on the heat transfer coefficient was rather small. In this test series, the heat flux was either 10 or 20 kW/m². The heat transfer coefficient varied less than 1 to 2% as a result of varying heat flux. The measured values show a high accuracy compared with the calculated results. From Gnielinski's correlation one can find an explanation of the (negligible) influence of the heat flux on the heat transfer coefficient; The influence is taken into account by means of the correction factor (Pr/Prw)0.11. Since the wall temperature changes with the heat flux, the Prandtl number at the wall temperature (Prw) changes as well. However, due to the small exponent of 0.11 the correction factor is almost 1 for the test conditions applied.

Gascooling inside the microchannel tube

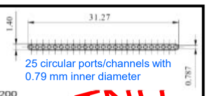

25 circular ports/channels with 0.79 mm inner diameter

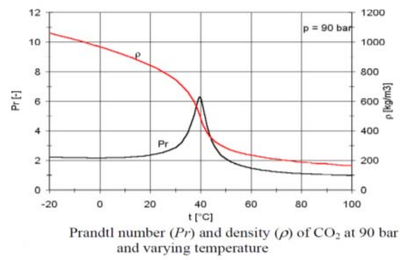

Prandtl number (Pr) and density (ρ) of CO_2 at 90 bar and varying temperature

Influence of the pressure on the heat transfer coefficient (80-100 bar)

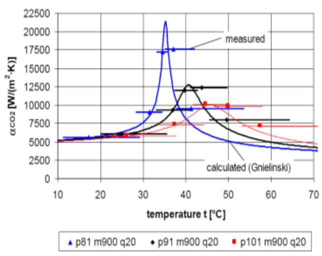

Since the heat transfer coefficient reaches a maximum at the pseudocritical temperature, this maximum will change with varying pressure. As may be observed, **the max-imum heat transfer coefficient increases when the pressure approaches the critical pressure of CO_2** (73.8 bar).

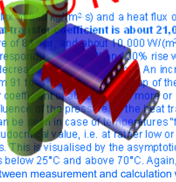

For a mass flux [illegible] kg/(m²·s) and a heat flux of 20 kW/m², the **peak heat transfer coefficient is about 21,000 W/(m²K)** for a pressure of 8[illegible], and about 10,000 W/(m²K) at 101 bar. This correspond[illegible] [illegible]0% rise when the pressure is decrea[illegible] An increase of the pressure from 91 to [illegible] of the maximum heat transfer coeffi[illegible] more or less negligible influence of the pressure [illegible] the heat transfer coefficient can be seen in case of temperatures "far away" from the pseudocritical value, i.e. at rather low or high temperatures. This is visualised by the asymptotic approach of the curves below 25°C and above 70°C. Again, the deviation between measurement and calculation was small.

Measurements versus correlations

$$\sigma_{avg} = \frac{l}{n}\sum_{n}\frac{(\alpha_{calc}-\alpha_{meas})}{\alpha_{meas}} \quad \text{... average deviation}$$

$$\sigma_{mean} = \frac{l}{n}\sum_{n}\left|\frac{(\alpha_{calc}-\alpha_{meas})}{\alpha_{meas}}\right| \quad \text{... mean deviation}$$

Deviation between measured heat transfer coefficients and calculation models

	σ_{avg} [%]	σ_{mean} [%]
simple Gnielinski	-3	4
Gnielinski	-1	4
Gnielinski (VDI)	-7	8
Polyakov	19	19
Ghajar & Asadi	1	8
Dittus-Boelter (n = 1/3)	-18	18
Dittus-Boelter (n = 0.4)	-7	9

"simple Gnielinski" means Gnielinski's correlation for the Nusselt number using the Haaland (1983) friction factor and neglecting the influence of the wall temperature (see above). The other variant of the original Gnielinski correlation was "Gnielinski (VDI)" where the Filonenko (1954) friction factor was used.

Gnielinski's correlation VDI (1994):

$$Nu_m = \frac{\frac{f}{8}\cdot(Re-1000)\cdot Pr}{1+12.7\cdot\sqrt{\frac{f}{8}}\cdot(Pr^{2/3}-1)}\cdot\left[1+\left(\frac{d}{l}\right)^{2/3}\right]$$

l is the tube length, and f is the pressure drop factor.

Haaland's friction factor

$$f = \left\{-1.8\cdot log\left[\frac{6.9}{Re}+\left(\frac{\varepsilon/d}{3.7}\right)^{1.11}\right]\right\}^{-2}$$

ε is the tube roughness.

Influence of the pressure [80-90-100 bar] on the pressure drop (Δl_{tube} = 503 mm)

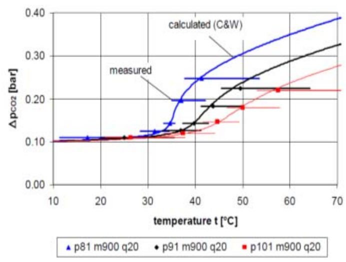

Since the **pressure has a large influence on the pseudocritical temperature**, the pressure-drop characteristics **change with the absolute value of the pressure**.
If the pressure changes from 91 to 81 bar and from 91 to 101 bar, the mean pressure drop changes about +17% and -13%, respectively, in the temperature range 10 to 70°C.

The corresponding change of the heat transfer coefficient was +68 and -20%, respectively.

Influence of the mass flux [600-900-1200 kg/(m²s)] on the pressure drop (Δl_{tube} = 503 mm)

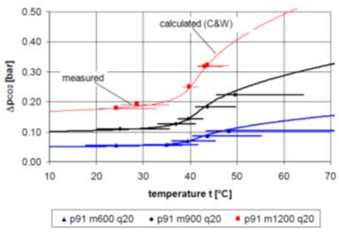

For the single-phase pressure drop: VDI (heat atlas) recommends the implicit form for the friction factor according to Colebrook & White:

$$\frac{1}{\sqrt{f}} = -2\cdot log\left[\frac{2.51}{Re\cdot\sqrt{f}}+\frac{\varepsilon/d}{3.71}\right]$$

As expected the mass flow rate influences the pressure drop considerably. In case of an increase of the mass flux from 600 to 900kg/(m²s) and from 600 to 1200 kg/(m²s), the measured pressure drop increased by about 100% and 240%, respectively.

As stated before, the heat transfer coefficient increased by about 40% and 80%, respectively, at the same conditions.

Summary 'gascooling' with micro channels

- In a transcritical cycle, the **refrigerant is cooled down at a supercritical pressure**. In this region the influence of the critical point on the properties is large. This fact leads to conditions in CO_2 equipment differing considerably from in systems using conventional refrigerants.
- The experimental **results confirm that CO_2 offers high heat transfer coefficients at supercritical pressures**. A comparison between experimental data and common correlations showed an acceptable correspondence. Especially the *Nusselt number* based on *Gnielinski's* correlation in combination with *Haaland's friction factor* correlated the experimental heat transfer data well.
- The expected pressure drop of CO_2 in a refrigerant cooler is rather high, but **due to the high pressure level, the effect on temperature loss is moderate**. A comparison between experimental and calculated results according to the *Colebrook & White* correlation showed a satisfactory agreement.

Influence of the heat flux [10 or 20 kW/m²] on the pressure drop (Δl_{tube} = 503 mm)

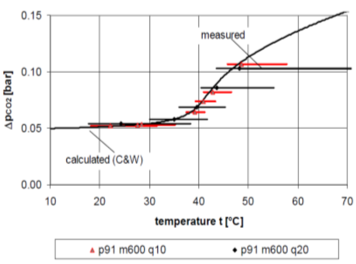

Npressure drop. In general, the influence of varying temperature on pressure drop changes significantly close to the pseudocritical temperature.
The steep gradient is caused by the rapid change in CO_2-density in this region,

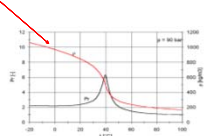

Figure 2: Prandtl number (Pr) and density (ρ) of CO_2 at 90 bar and varying temperature

Flow maldistribution (Results from Vist, 2004)

- Distribution of flow into parallel flowhannels
  - between tubes in a manifold
  - between parallel ports in a tube
- Non-uniform distribution of single-phase flow
- Separation of two-phase flow in manifold
- Reduced performance
- Uneven frosting

R-134a, G = 120/330 kgm⁻²s⁻¹ (manifold/tubes), x in = 0.2

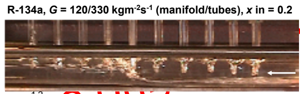

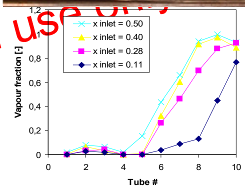

Experimental test rig

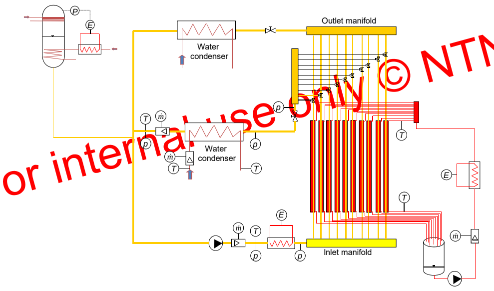

Conclusions maldistribution

- Experimental measurements:
  - Severe maldistribution of both phases: Vapour entering the first tubes and liquid entering the last tubes
  - The ID8 mm manifold showed improved distribution
- Literature T-junction correlations:
  - Good predictions of 16 mm manifold data
  - Larger deviations compared to 8 mm manifold data
- Low manifold mass flux: correlation between branch vapour fraction and manifold vapour mass flux
- High manifold mass flux: constant liquid take-off fraction
- **The tested manifold can be analysed as a series of T-junctions**

Test section

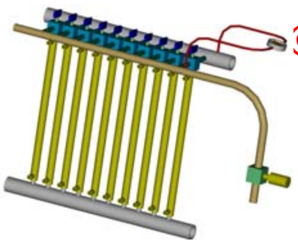

Examples of heat exchanger designs

Manifolds, round tube and multiport tube (MPE)

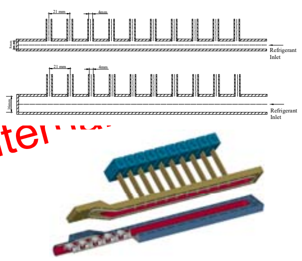

ECO Group - Tube-in-fin

www.ecogroup.com

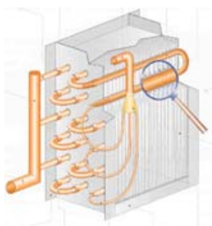

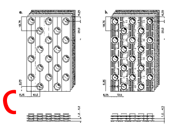

Consept 712:

Tube OD	7.2 mm
Fin spacing	1.2 ... 4.2 mm
Vertical tube spacing	25 mm
Horizontal tube spacing	12.5
Tube configuration	Staggered

Consept 722 (Chages compared to 712):

Fin spacing	1.4 ... 6.0mm
Horizontal tube spacing	21.65 mm

BEHR Industrietechnik - Tube-in-fin

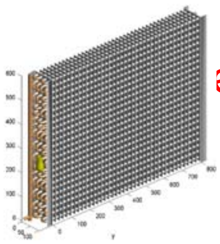

Example:

Tube OD	8.44 mm
Fin spacing	3 mm
Vertical tube spacing	25 mm
Horisontal tube spacing	25 mm
Tube configuration	In-line

Plate in Shell

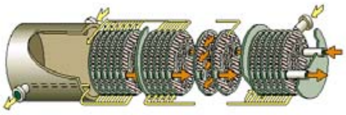

- Capacity 5 to 100 000 kW/unit
- Design Temperature – 200°C to + 900°C
- Design Pressure Standard design 16, 25 and 40 bar up to 100 bar

VAHTERUS

Multiport Extruded Tubes - MPE

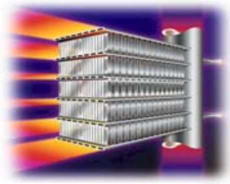

Advantages:
- **Compact**
- **Low cost for larger series**

Disadvantages:
- **Defrosting and water shedding may be a challenge**

Components for MPE heat exchangers:
Hydro Aluminium

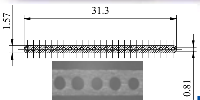

Tube-in-shell

Advantages:
- **All capacities**
- **Several manufactuterers**

Disadvantages:
- **Large volumes**
- **Heavy**

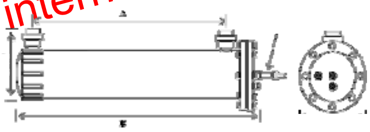

Tube-in-tube

EXERGY, LLC

Printed Circuits

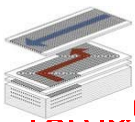

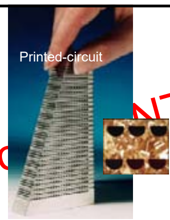

- **Capacity: According to design**
- **Design Temperature: Cryo to + 900°C**
- **Design Pressure up to 500 bar**

HEATRIC

www.heatric.com

Why internal heat exchanger?

- Ensures superheated gas to the compressor
  - To avoid liquid slugging
  - Increased compressor efficiencies
- Increased cooling capacities at high ambient temperatures

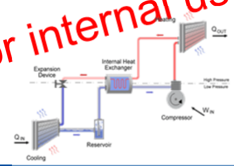

- Reduced optimal high pressure
- Increased energy efficiency at high ambient temperatures

Different types of internal heat exchangers (IHX) have been developed

- Tube-in-tube
- "Star" in tube
- Brazed MPE tube type
- Soldered tube-by-tube

Internal Heat Exchange (Mobile A/C)

From U of I - Pega Hrnjak

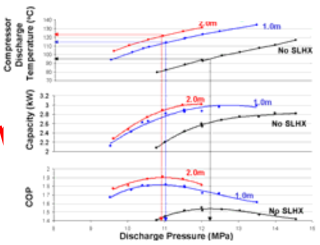

Idling
43°C
ambient

Application of an IHX (water heat pump 10°C → 60°C)

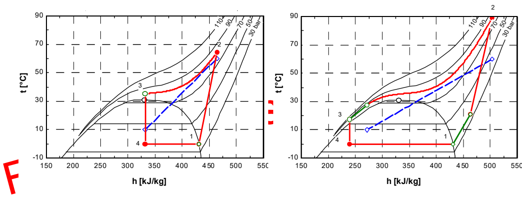

⇒ IHX may damp the influence of high-side pressure on COP & increases capacity

Examples of Internal heat exchanger designs

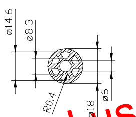

Extruded tube counterflow type

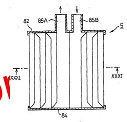

Fig.31

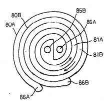

Coiled counterflow type
(Sakakibara et al., 1997 Eur. Pat. Appl.)